IMA Journal of Numerical Analysis (2018) **00**, 1–24
doi:10.1093/imanum/dry021

Two low-order nonconforming finite element methods for the Stokes flow in three dimensions

Jun Hu
LMAM and School of Mathematical Sciences, Peking University, Beijing 100871, P. R. China
hujun@math.pku.edu.cn

and

Mira Schedensack*
Institut für Numerische und Angewandte Mathematik, Universität Münster, Einsteinstr. 62, D-48149 Münster, Germany
*Corresponding author: mira.schedensack@uni-muenster.de

[Received on 18 October 2017; revised on 14 March 2018]

In this paper, we propose two low-order nonconforming finite element methods (FEMs) for the three-dimensional Stokes flow that generalize the nonconforming FEM of Kouhia & Stenberg (1995, A linear nonconforming finite element method for nearly incompressible elasticity and Stokes flow. *Comput. Methods Appl. Mech. Eng*, **124**, 195–212). The finite element spaces proposed in this paper consist of two globally continuous components (one piecewise affine and one enriched component) and one component that is continuous at the midpoints of interior faces. We prove that the discrete Korn inequality and a discrete inf–sup condition hold uniformly in the mesh size and also for a nonempty Neumann boundary. Based on these two results, we show the well-posedness of the discrete problem. Two counterexamples prove that there is no direct generalization of the Kouhia–Stenberg FEM to three space dimensions: the finite element space with one nonconforming and two conforming piecewise affine components does not satisfy a discrete inf–sup condition with piecewise constant pressure approximations, while finite element functions with two nonconforming and one conforming component do not satisfy a discrete Korn inequality.

Keywords: nonconforming; finite element method; Korn's inequality; LBB condition; divergence-free.

1. Introduction

Given a polygonal, bounded Lipschitz domain $\Omega \subseteq \mathbb{R}^3$ with closed Dirichlet boundary Γ_D and Neumann boundary $\Gamma_N = \partial\Omega \setminus \Gamma_D$, both with positive two-dimensional measure, and some right-hand side $g \in \left[L^2(\Omega)\right]^3$, the three-dimensional Stokes problem seeks the velocity $u \in \left[H^1(\Omega)\right]^3$ and the pressure $p \in L^2(\Omega)$ with

$$\left.\begin{aligned} -2\mu \operatorname{div} \varepsilon(u) + \nabla p &= g \\ \operatorname{div} u &= 0 \end{aligned}\right\} \text{ in } \Omega, \quad u|_{\Gamma_D} = 0, \quad (2\mu\varepsilon(u) - pI_{3\times 3})|_{\Gamma_N} \nu = 0. \tag{1.1}$$

Here and throughout this paper, μ is the viscosity. The symmetric gradient of a vector field reads $\varepsilon(v) := 1/2\left(\nabla v + \nabla v^{\mathrm{T}}\right)$ for any $v \in \left[H^1(\Omega)\right]^3$, while ν denotes the outer unit normal.

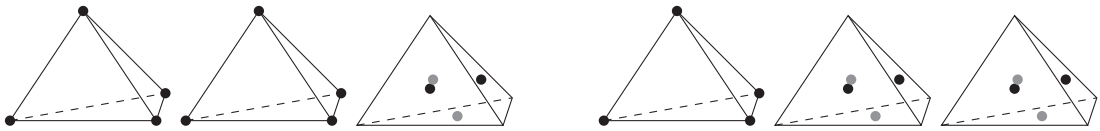

FIG. 1. Degrees of freedom of the velocity for the direct generalization of the two-dimensional FEM of Kouhia and Stenberg (Kouhia & Stenberg, 1995). The two FEMs are not stable, as shown in Section 4.

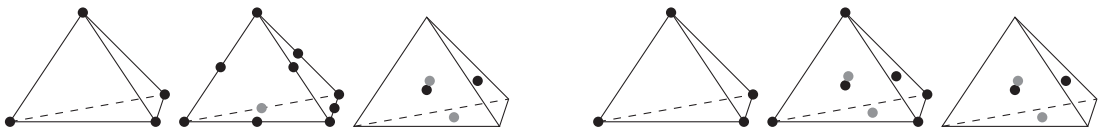

FIG. 2. Degrees of freedom of the velocity approximation for the two new stable finite elements. The pressure is approximated with piecewise constants.

Finite element methods (FEMs) for the two-dimensional Stokes problem have been extensively studied in the literature; most of stable schemes are summarized in the book by Boffi *et al.* (2013). However, only a little attention has been paid to the three-dimensional problem. Here we only mention the works by Stenberg (1987), Boffi (1997), Zhang (2005), Guzmán & Neilan (2014) and Neilan & Sap (2016) for the three-dimensional Taylor–Hood elements. FEMs with discontinuous ansatz functions for the pressure, and therefore, an improved mass-conservation, are introduced in the studies by Bernardi & Raugel (1985), Boffi *et al.* (2012a, 2012b). If $\Gamma_N = \emptyset$, the Stokes equations can be reformulated in terms of the full gradient of u. In this case, the nonconforming FEM of Crouzeix & Raviart (1973) yields a stable approximation. Otherwise, it is not stable due to a missing Korn inequality in two as well as in three dimensions. In two dimensions, the nonconforming FEM of Kouhia & Stenberg (1995) circumvents this by choosing only one component nonconforming and the other one conforming. This nonconforming FEM is the lowest-order FEM for the Stokes problem with piecewise constant pressure approximation in two dimensions. A generalization to higher polynomial degrees of that FEM can be found in the study by Schedensack (2017).

One key result of this paper consists of two counterexamples in Section 4 below which imply that a generalization to three dimensions with two conforming and one nonconforming component is not inf–sup stable, while a generalization with one conforming and two nonconforming components does not satisfy a discrete Korn inequality; see Fig. 1 for a visualization of the degrees of freedom for those two FEMs. To ensure both a discrete inf–sup stability and a discrete Korn inequality, we employ a discrete space consisting of one piecewise affine and globally continuous and one nonconforming piecewise affine component. The third component can be approximated in the space of piecewise quadratic and globally continuous functions, as well as in the space of piecewise affine and globally continuous functions enriched with face bubble functions; see Fig. 2 for an illustration of the degrees of freedom. The discrete inf–sup condition and the discrete Korn inequality imply the well-posedness of the method. Furthermore, the recently established medius analysis technique (Gudi, 2010; Badia *et al.*, 2014; Hu *et al.*, 2014; Carstensen *et al.*, 2015; Carstensen & Schedensack, 2015) together with the *a posteriori* techniques of Carstensen (2005) and Carstensen & Hu (2007) proves a best-approximation result for the nonconforming FEM; see Theorem 3.13 below.

The rest of the paper is organized as follows. In Section 2, we present the FEM for (1.1). The well-posedness of the discrete problem will be proved in Section 3. Two counterexamples are given in

Section 4 which prove that discretizations with piecewise affine approximations for the velocity and piecewise constant approximations for the pressure are not stable. Section 5 concludes the paper with numerical experiments.

Throughout this paper, standard notation on Lebesgue and Sobolev spaces is employed and $(\bullet, \bullet)_{L^2(\Omega)}$ denotes the L^2 scalar product over Ω. Let $\| \bullet \|_{0,\omega}$ denote the L^2 norm over a set $\omega \subseteq \Omega$ (possibly two-dimensional) and $\| \bullet \|_0$ abbreviates $\| \bullet \|_{0,\Omega}$. The space $H^1_D(\Omega)$ consists of all H^1 functions that vanish on Γ_D in the sense of traces. Let $A \lesssim B$ abbreviate that there exists some mesh-size-independent generic constant $0 \leq C < \infty$ such that $A \leq CB$ and let $A \approx B$ abbreviate $A \lesssim B \lesssim A$.

2. FEM

Suppose that the closure $\overline{\Omega}$ is covered exactly by a regular and shape-regular triangulation $\mathcal{T}$ of $\overline{\Omega}$ into closed tetrahedra in three dimensions in the sense of Ciarlet (Brenner & Scott, 2008), that is, two distinct tetrahedra are either disjoint or share exactly one vertex, edge or face. Let $\mathcal{F}$ denote the set of all faces in $\mathcal{T}$ with $\mathcal{F}(\Omega)$ the set of interior faces, $\mathcal{F}(\Gamma_D)$ the set of faces on Γ_D and $\mathcal{F}(\Gamma_N)$ the set of faces on Γ_N. Let $\mathcal{N}$ be the set of all vertices with $\mathcal{N}(\Omega)$ the set of interior vertices, $\mathcal{N}(\Gamma_D)$ the set of vertices on Γ_D and $\mathcal{N}(\Gamma_N)$ the set of vertices on Γ_N. The set of faces of the element T is denoted by $\mathcal{F}(T)$. By h_T we denote the diameter of the element $T \in \mathcal{T}$ and by $h_{\mathcal{T}}$ the piecewise constant mesh-size function with $h_{\mathcal{T}}|_T = h_T$ for all $T \in \mathcal{T}$. We denote by ω_T the union of (at most five) tetrahedra $T' \in \mathcal{T}$ that share a face with T and by ω_F the union of (at most two) tetrahedra having in common the face F. Given any face $F \in \mathcal{F}(\Omega)$ with diameter h_F we assign one fixed unit normal $\nu_F := (\nu_1, \nu_2, \nu_3)$. For F on the boundary we choose $\nu_F = \nu$ the unit outward normal to Ω. Once ν_F has been fixed on F, in relation to ν_F one defines the elements $T_- \in \mathcal{T}$ and $T_+ \in \mathcal{T}$, with $F = T_+ \cap T_-$ and $\omega_F = T_+ \cup T_-$, such that ν_F is the outward normal of T_+. Given $F \in \mathcal{F}(\Omega)$ and some $\mathbb{R}^d$-valued function v defined in Ω, with $d = 1$, 2, 3, we denote by $[v] := (v|_{T_+})|_F - (v|_{T_-})|_F$ the jump of v across F which will become the trace on boundary faces.

Let $P_0(T)$ denote the space of constant functions on T, $P_1(T)$ the space of affine functions and $P_2(T)$ the space of quadratic functions and let $S^{\mathrm{C},1}_D$ and $S^{\mathrm{C},2}_D$ denote the piecewise affine and piecewise quadratic conforming finite element spaces over $\mathcal{T}$ which are written

$$S^{\mathrm{C},1}_D := \left\{ v \in H^1_D(\Omega) \,\middle|\, \forall\, T \in \mathcal{T},\ v|_T \in P_1(T) \right\},$$
$$S^{\mathrm{C},2}_D := \left\{ v \in H^1_D(\Omega) \,\middle|\, \forall\, T \in \mathcal{T},\ v|_T \in P_2(T) \right\}.$$

The nonconforming linear finite element space $S^{\mathrm{NC},1}_D$ is defined as

$$S^{\mathrm{NC},1}_D := \left\{ v \in L^2(\Omega) \,\middle|\, \begin{array}{l} \forall\, T \in \mathcal{T},\ v|_T \in P_1(T),\ \forall\, F \in \mathcal{F}(\Omega),\ \int_F [v]_F \,\mathrm{d}s = 0 \\ \text{and } \forall\, F \in \mathcal{F} \text{ with } F \subseteq \Gamma_D,\ \int_F v \,\mathrm{d}s = 0 \end{array} \right\}.$$

Define also the space of face bubbles by

$$\mathcal{B}_{\mathcal{F}} := \mathrm{span}\{\varphi_F | F \in \mathcal{F}(\Omega) \text{ or } F \in \mathcal{F} \text{ with } F \subseteq \Gamma_N\}$$

with the face bubbles $\varphi_F \in H^1_D(\Omega)$ defined by

$$\varphi_F := 60\lambda_a\lambda_b\lambda_c \quad \text{for} \quad F = \operatorname{conv}\{a,b,c\}$$

and with barycentric coordinates $\lambda_a, \lambda_b, \lambda_c$. We consider two finite element spaces for the velocity. The first one is the space that contains second-order polynomials in the second component and it is defined by

$$V_{2,D} := S^{\mathrm{C},1}_D \times S^{\mathrm{C},2}_D \times S^{\mathrm{NC},1}_D.$$

As a second finite element space for the velocity we consider the enrichment of the second component by face bubbles, i.e.,

$$V_{\mathcal{F},D} := S^{\mathrm{C},1}_D \times \left(S^{\mathrm{C},1}_D + \mathcal{B}_{\mathcal{F}}\right) \times S^{\mathrm{NC},1}_D.$$

Since $V_{2,D}$ and $V_{\mathcal{F},D}$ are nonconforming spaces, the differential operators ∇, ε and div are defined elementwise, written as ∇_h,ε_h and div_h, respectively. We equip the space $V_{2,D}$ and $V_{\mathcal{F},D}$ with the broken norm

$$\|v\|^2_{1,h} := \|v\|^2_0 + \|\nabla_h v\|^2_0 \quad \text{for all } v \in V_{2,D} \oplus V_{\mathcal{F},D}\,.$$

For both choices of finite element spaces for the velocity, the pressure will be sought in the space

$$Q_h := \left\{q \in L^2(\Omega) | \forall\, T \in \mathcal{T},\ q|_T \in P_0(T)\right\}$$

consisting of piecewise constant functions. Let $V_{h,D}$ be $V_{2,D}$ or $V_{\mathcal{F},D}$. The FEM then reads as follows: find $u_h \in V_{h,D}$ and $p_h \in Q_h$ with

$$\begin{aligned} a_h(u_h, v_h) + b_h(v_h, p_h) &= (g, v_h)_{L^2(\Omega)} && \text{for all } v_h \in V_{h,D}, \\ b_h(u_h, q_h) &= 0 && \text{for all } q_h \in Q_h, \end{aligned} \tag{2.1}$$

where the two discrete bilinear forms are written

$$\begin{aligned} a_h(u_h, v_h) &:= 2\mu \int_\Omega \varepsilon_h(u_h) : \varepsilon_h(v_h)\,\mathrm{d}x, \\ b_h(v_h, p_h) &:= -\int_\Omega p_h \operatorname{div}_h v_h\,\mathrm{d}x. \end{aligned}$$

The next section proves a discrete inf–sup condition and a discrete Korn inequality. Those two ingredients then imply the existence of a unique solution from Corollary 3.12 and the best-approximation error estimate of Theorem 3.13 below. This leads to the convergence against the solution of the (weak form of) (1.1), namely the solution $(u,p) \in \left[H^1_D(\Omega)\right]^3 \times L^2(\Omega)$ with

$$\begin{aligned} 2\mu(\varepsilon(u), \varepsilon(v))_{L^2(\Omega)} - (p, \operatorname{div} v)_{L^2(\Omega)} &= (g, v)_{L^2(\Omega)} && \text{for all } v \in \left[H^1_D(\Omega)\right]^3, \\ (q, \operatorname{div} u)_{L^2(\Omega)} &= 0 && \text{for all } q \in L^2(\Omega). \end{aligned} \tag{2.2}$$

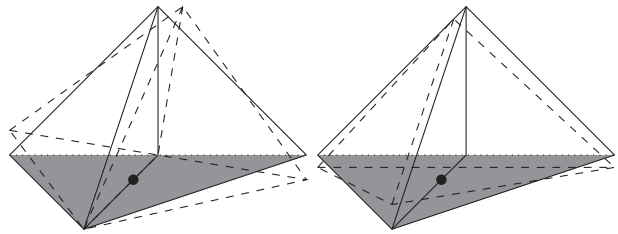

FIG. 3. Two infinitesimal rigid body motions that satisfy the Dirichlet boundary conditions at the gray face in the nonconforming sense.

3. The stability analysis

In this section, we prove the well-posedness of the discrete problem and a best-approximation result, which follow from the discrete Korn inequality and the inf–sup condition from Theorems 3.9 and 3.10 below.

The discrete Korn inequality relies on the following assumption.

ASSUMPTION 3.1 Any face $F \in \mathcal{F}$ that lies on the Dirichlet boundary $F \subseteq \Gamma_D$, and that is horizontal in the sense that $|\nu_F(3)| = 1$, satisfies one of the following conditions:

(a) There exist a vertex $z \in \mathcal{N}$ and a face $F' \in \mathcal{F} \setminus \{F\}$ such that $z \in F \cap F'$, $F' \subseteq \Gamma_D$ and F' is not horizontal in the sense that $|\nu_{F'}(3)| < 1$.

(b) There exist a vertex $z \in \mathcal{N}$ and two faces $F', F'' \in \mathcal{F}$, $F' \neq F''$, such that $F' \subseteq \Gamma_D$, $F'' \subseteq \Gamma_D$ and $\{z\} = F \cap F' \cap F''$.

Note that in condition (b) all of the faces F, F' and F'' might be horizontal.

REMARK 3.2 Assumption 3.1 basically excludes that there are horizontal faces on the Dirichlet boundary that are surrounded by the Neumann boundary. If Assumption 3.1 is not satisfied, the triangulation can be refined with, e.g., a bisection algorithm such that vertices that satisfy condition (b) are created. Note that Assumption 3.1 is conserved by a red, green or bisection refinement.

Assumption 3.1 excludes the situation depicted in Fig. 3, where an infinitesimal rigid body motion is not excluded by the Dirichlet boundary condition, due to the nonconformity in the ansatz space.

REMARK 3.3 A permutation of the conforming, nonconforming and enriched finite element spaces in the definition of $V_{2,D}$ and $V_{\mathcal{F},D}$ is possible as well. The condition on horizontal faces in Assumption 3.1 has then to be replaced by the corresponding condition on vertical faces with $|\nu_F(1)| = 1$ or $|\nu_F(2)| = 1$, corresponding to the chosen nonconforming component. This might be beneficial in some situations.

We furthermore make the following Assumption 3.4.

ASSUMPTION 3.4 There exists no interior face $F \in \mathcal{F}(\Omega)$ whose three vertices lie on the boundary $\partial\Omega$. Furthermore, the triangulation $\mathcal{T}$ consists of more than one simplex.

REMARK 3.5 Similar assumptions to 3.1 and 3.4 are necessary for the two-dimensional situation. Assumption 3.1 is hidden in the study by Kouhia & Stenberg (1995) in the assumption that the mesh size has to be small enough. See also the study by Carstensen & Schedensack (2015) for a discussion about necessary conditions on the triangulation.

We define the set

$$\mathcal{N}(H1) := \left\{ z \in \mathcal{N}(\Gamma_D) \;\middle|\; \begin{array}{l} \exists\, F \in \mathcal{F} \text{ such that } F \subseteq \Gamma_D, |v_F(3)| = 1 \\ \text{and } z \text{ satisfies condition (a) or (b) for that } F \end{array} \right\}.$$

Furthermore, given any vertex $z \in \mathcal{N}(\Omega)$, we define

$$\mathcal{F}_z := \left\{ F \in \mathcal{F} \;\middle|\; \begin{array}{l} z \in F \text{ or } F \subseteq \Gamma_D \text{ with } |v_F(3)| < 1 \\ \text{and } \exists\, T \in \mathcal{T} \text{ with } z \in T \text{ and } F \subseteq T \end{array} \right\}$$

and for $z \in \mathcal{N}(H1)$ we let

$$\mathcal{F}_z := \{F \in \mathcal{F} \mid z \in F\}$$

denote the set of faces that share z.

REMARK 3.6 Assumptions 3.1 and 3.4 guarantee that any face $F \in \mathcal{F}(\Omega) \cup \mathcal{F}(\Gamma_D)$ is contained in a set $\mathcal{F}_z$ for some node $z \in \mathcal{N}(\Omega) \cup \mathcal{N}(H1)$.

To establish the discrete Korn inequality, we need the following key result. Let ω_z denote the patch of z, i.e.,

$$\omega_z := \operatorname{int}\left(\bigcup \{T \in \mathcal{T} | z \in T\}\right).$$

LEMMA 3.7 Let Assumptions 3.1 and 3.4 be satisfied. Let $V_{h,D}$ be the finite element space $V_{2,D}$ or $V_{\mathcal{F},D}$ and let $v_h \in V_{h,D}$. For any vertex $z \in \mathcal{N}(\Omega) \cup \mathcal{N}(H1)$, it holds that

$$\sum_{F \in \mathcal{F}_z} h_F^{-1} \|[v_h]_F\|_{0,F}^2 \leq C \inf_{v \in [H_D^1(\omega_z)]^3} \|\varepsilon_h(v - v_h)\|_{0,\omega_z}^2, \tag{3.1}$$

where

$$H_D^1(\omega_z) := \left\{ v \in H^1(\omega_z) \mid v = 0 \text{ on } \partial\omega_z \cap \Gamma_D \right\}.$$

The constant C may depend on the angles of the simplices and on the configuration of the simplices in ω_z, but it is independent of the mesh size.

Proof. In fact, both sides of (3.1) define seminorms for the restriction of v_h to ω_z. Suppose

$$\inf_{v \in [H_D^1(\omega_z)]^3} \|\varepsilon_h(v - v_h)\|_{0,\omega_z} = 0.$$

This implies

$$v_h = v + \mathrm{RM}_z$$

for some $v \in \left[H_D^1(\omega_z)\right]^3$ and some piecewise rigid body motion RM_z which is of the form

$$\mathrm{RM}_z|_T(x) := \begin{pmatrix} a_T - e_T x_2 - d_T x_3 \\ b_T + e_T x_1 - f_T x_3 \\ c_T + d_T x_1 + f_T x_2 \end{pmatrix} \quad \text{for any } T \in \mathcal{T} \text{ with } z \in T$$

for parameters $a_T, b_T, c_T, d_T, e_T, f_T$. Assumption 3.4 guarantees that ω_z consists of more than one simplex. Therefore, consider a face $F \in \mathcal{F}$ such that $F = T_1 \cap T_2$ for some $T_k \in \mathcal{T}$, $T_k \subseteq \omega_z$ for $k = 1, 2$ and F is not horizontal, i.e., $|\nu_F(3)| < 1$. Then there exist parameters $\alpha, \beta, \gamma \in \mathbb{R}$ such that w.l.o.g.,

$$F \subseteq \left\{ x \in \mathbb{R}^3 \mid x_1 + \alpha x_2 + \beta x_3 = \gamma \right\}.$$

Since the first two components of v_h are continuous across internal faces, it follows that

$$\begin{aligned} (a_{T_1} - a_{T_2}) - (e_{T_1} - e_{T_2})x_2 - (d_{T_1} - d_{T_2})x_3 = 0, \\ (b_{T_1} - b_{T_2}) + \gamma(e_{T_1} - e_{T_2}) - \alpha(e_{T_1} - e_{T_2})x_2 - (f_{T_1} - f_{T_2} + \beta(e_{T_1} - e_{T_2}))x_3 = 0. \end{aligned}$$

Since this holds for all $x_2, x_3 \in \mathbb{R}$, this leads to

$$a_{T_1} = a_{T_2}, \quad b_{T_1} = b_{T_2}, \quad d_{T_1} = d_{T_2}, \quad e_{T_1} = e_{T_2}, \quad f_{T_1} = f_{T_2}.$$

Note that the integral mean of the last component of v_h is continuous across F. This leads to

$$c_{T_1} = c_{T_2}.$$

We conclude that RM_z is continuous across any face F that is not horizontal. The same arguments prove that $\mathrm{RM}_z|_T$ vanishes if T contains a face $F \subseteq \Gamma_D$ that is not horizontal.

To conclude that RM_z is continuous on the whole patch ω_z, we let $\mathcal{F}_{z,H}$ denote the set of faces in $\mathcal{F}_z$ that are horizontal and consider the following cases.

Case 1: $\mathcal{F}_{z,H} = \emptyset$. In this case, RM_z is clearly continuous on ω_z.

Case 2: $z \in \mathcal{N}(\Omega)$ and $\mathcal{F}_{z,H} \neq \emptyset$. Let $D_\delta(z)$ denote the disk with radius δ and center z, i.e.,

$$D_\delta(z) := \{x \in \omega_z \mid (x - z) \cdot (0, 0, 1) = 0 \text{ and } |x - z| < \delta\}.$$

We first consider the case that the faces in $\mathcal{F}_{z,H}$ do not cover a whole disk, i.e., $D_\delta(z) \not\subseteq \bigcup \mathcal{F}_{z,H}$ for all $\delta > 0$. Then $\omega_z \setminus \bigcup \mathcal{F}_{z,H}$ is still connected and it follows that RM_z is continuous.

If the faces in $\mathcal{F}_{z,H}$ contain a whole disk centered at z, i.e., there exists some $\delta > 0$ such that $D_\delta(z) \subseteq \bigcup \mathcal{F}_{z,H}$, then the set ω_z is divided into two parts by the faces of $\mathcal{F}_{z,H}$. Let $\mathcal{F}^i_{z,H} \subseteq \mathcal{F}_{z,H}$ denote the set of those separating faces in $\mathcal{F}_{z,H}$ that are all faces that are not on Γ_D. In each part, RM_z restricted to one of these parts is a global rigid body motion. The set $\mathcal{F}^i_{z,H}$ contains at least three faces because z is an interior vertex. Since the jump across $\bigcup \mathcal{F}^i_{z,H}$ of the third component of RM_z is an affine function and vanishes at least at three different points that are not collinear, we have that RM_z is continuous.

If there exists some face $F \in \mathcal{F}_z$ with $F \subseteq \Gamma_D$, then this face is not horizontal by the definition of $\mathcal{F}_z$ for interior nodes. Therefore, RM_z vanishes.

Case 3: $z \in \mathcal{N}(H1)$ with z from (a) from Assumption 3.1. In this case, $\mathcal{F}_z$ contains a face $F' \in \mathcal{F}_z$ with $F' \subseteq \Gamma_D$ that is not horizontal. Therefore, RM_z vanishes.

Case 4: $z \in \mathcal{N}(H1)$ with z from (b) from Assumption 3.1. In this case, there exist at least three faces $F, F', F'' \in \mathcal{F}_z$, which lie on the Dirichlet boundary and are horizontal. Since the jump

across $\bigcup \mathcal{F}_{z,H}$ of the third component of RM_z is an affine function and vanishes at least at the midpoints of these faces, we have that RM_z vanishes.

In all of the above cases, RM_z is continuous on ω_z and vanishes if $\mathcal{F}_z$ contains Dirichlet boundary faces. If $F \in \mathcal{F}_z$ and $F \not\subseteq \Gamma_D$, then $\mathrm{int}(F) \subseteq \omega_z$ for the relative interior $\mathrm{int}(F)$ of F. Therefore,

$$\sum_{F\in\mathcal{F}_z} h_F^{-1}\|[v_h]_F\|_{0,F}^2 = 0.$$

In other words, the left-hand side of (3.1) vanishes. Hence, the two seminorms of the left and right side of (3.1) satisfy

$$\sum_{F\in\mathcal{F}_z} h_F^{-1}\|[v_h]_F\|_{0,F}^2 \le C \inf_{v\in[H^1_D(\omega_z)]^3} \|\varepsilon_h(v-v_h)\|_{0,\omega_z}^2.$$

A scaling argument shows that C is independent of the mesh size. □

Remark 3.8 Note that the proof of Lemma 3.7 has to control only piecewise rigid body motions and, therefore, the proof (and, hence, also Theorem 3.9 below) holds true for any choice of finite element space for the first and second components as long as they are conforming.

With this lemma, we are in a position to prove the discrete Korn inequality.

Theorem 3.9 Assume that Assumptions 3.1 and 3.4 hold and that $h_F \lesssim 1$ for all $F \in \mathcal{F}(\Gamma_D)$. Let $V_{h,D}$ be $V_{2,D}$ or $V_{\mathcal{F},D}$. There exists a positive constant β independent of the mesh size such that

$$\beta\|v_h\|_{1,h} \le \|\varepsilon_h(v_h)\|_0 \qquad \text{for all } v_h \in V_{h,D}.$$

Proof. The discrete Poincarè inequality from the study by Brenner (2003, (1.5)) implies

$$\|v_h\|_0^2 \lesssim \|\nabla_h v_h\|_0^2 + \left|\int_{\Gamma_D} v_h\,\mathrm{d}s\right|^2 \lesssim \|\nabla_h v_h\|_0^2 + \sum_{F\in\mathcal{F}(\Gamma_D)} h_F^{-1}\|v_h\|_{0,F}^2$$

provided $h_F \lesssim 1$ for all $F \in \mathcal{F}(\Gamma_D)$. The discrete Korn inequality from the study by Brenner (2004, (1.19)) then leads to

$$\begin{aligned}\|v_h\|_0^2 + \|\nabla_h v_h\|_0^2 &\le C\left(\|\varepsilon_h(v_h)\|_0^2 + \|v_h\|_{L^2(\Gamma_D)}^2 + \sum_{F\in\mathcal{F}(\Omega)\cup\mathcal{F}(\Gamma_D)} h_F^{-1}\|[v_h]_F\|_{L^2(F)}^2\right)\\ &\lesssim C\left(\|\varepsilon_h(v_h)\|_0^2 + \sum_{F\in\mathcal{F}(\Omega)\cup\mathcal{F}(\Gamma_D)} h_F^{-1}\|[v_h]_F\|_{L^2(F)}^2\right).\end{aligned}$$

Lemma 3.7 and Remark 3.6 then yield the assertion. □

For the proof of the inf–sup condition, define for any interior vertex z the associated macro-element by

$$\mathcal{M} = \mathcal{M}(z) = \{T \in \mathcal{T} \mid z \in T\}$$

and let

$$\Omega_{\mathcal{M}} = \operatorname{int}\left(\bigcup \mathcal{M}\right).$$

Furthermore, define the bilinear form $\mathcal{B}$ for all $v_h \in V_{2,D} \cup V_{\mathcal{F},D}$ and $q_h \in Q_h$ by

$$\mathcal{B}(u_h, p_h; v_h, q_h) := a_h(u_h, v_h) + b_h(v_h, p_h) - b_h(u_h, q_h)$$

and the norm

$$|\!|\!|(v_h, q_h)|\!|\!|_h^2 := \|\nabla_h v_h\|_{L^2(\Omega)}^2 + \|q_h\|_{L^2(\Omega)}^2.$$

THEOREM 3.10 Let $V_{h,D}$ be $V_{2,D}$ or $V_{\mathcal{F},D}$. If Assumptions 3.1 and 3.4 are satisfied, then there exists a positive constant α independent of the mesh size, such that

$$\sup_{(v_h, q_h) \in (V_{h,D} \times Q_h) \setminus \{0\}} \frac{\mathcal{B}(u_h, p_h; v_h, q_h)}{|\!|\!|(v_h, q_h)|\!|\!|_h} \geq \alpha |\!|\!|(u_h, p_h)|\!|\!|_h \qquad \text{for all } (u_h, p_h) \in V_{h,D} \times Q_h.$$

Proof. The proof is divided into two steps.

Step 1. We use the macroelement trick from the study by Kouhia & Stenberg (1995). To this end, let $z \in \mathcal{N}(\Omega)$ be an interior node with macroelement $\mathcal{M}$. Define

$$\widetilde{V}_{0,\mathcal{M}} := \left\{ v \in [L^2(\Omega_{\mathcal{M}})]^3 \;\middle|\; \begin{array}{l} v = (v_1, v_2, v_3) \text{ with } v_1 \in H_0^1(\Omega_{\mathcal{M}}),\ v_2 \in H_0^1(\Omega_{\mathcal{M}}), \\ \forall\, T \in \mathcal{M}\,, \forall\, i = 1, 3 :\ v_i|_T \in P_1(T), \\ \int_F [v_3]\, \mathrm{d}s = 0 \text{ for any interior face } F \text{ of } \mathcal{M}, \\ \int_F v_3\, \mathrm{d}s = 0 \text{ for any face } F \subseteq \partial\Omega_{\mathcal{M}} \end{array} \right\},$$

$$Q_{\mathcal{M}} := \left\{ q \in L^2(\Omega_{\mathcal{M}}) \mid \forall\, T \in \mathcal{M},\ q|_T \text{ is constant} \right\},$$

$$N_{\mathcal{M}} := \left\{ q \in Q_{\mathcal{M}} \mid \forall\, v \in V_{0,\mathcal{M}} :\ \int_\Omega q \operatorname{div}_h v\, \mathrm{d}x = 0 \right\}.$$

In the case that $V_{h,D}$ equals $V_{2,D}$, let

$$V_{0,\mathcal{M}} := \left\{ v \in \widetilde{V}_{0,\mathcal{M}} \mid \forall\, T \in \mathcal{M}\,, v_2|_T \in P_2(T) \right\},$$

while in the case that $V_{h,D}$ equals $V_{\mathcal{F},D}$, we set

$$V_{0,\mathcal{M}} := \left\{ v \in \widetilde{V}_{0,\mathcal{M}} \mid \forall\, T \in \mathcal{M}\,, v_2|_T \in P_1(T) + \operatorname{span}\{\varphi_F \mid F \in \mathcal{F}(\Omega_{\mathcal{M}})\} \right\}.$$

Let $q \in N_{\mathcal{M}}$. Define for any F with $\nu_F(3) \neq 0$ a function $v \in V_{0,\mathcal{M}}$ by $v_1 = 0\,, v_2 = 0$, $\int_F v_3\, \mathrm{d}s = 1$ and $\int_{F'} v_3\, \mathrm{d}s = 0$ for any face $F' \neq F$. Then an integration by parts implies

$$0 = \int_{\omega_z} q \operatorname{div}_h v\, \mathrm{d}x = \int_{T_+} \frac{\partial v_3}{\partial x_3} q|_{T_+}\, \mathrm{d}x + \int_{T_-} \frac{\partial v_3}{\partial x_3} q|_{T_-}\, \mathrm{d}x = v_3(q|_{T_+} - q|_{T_-}).$$

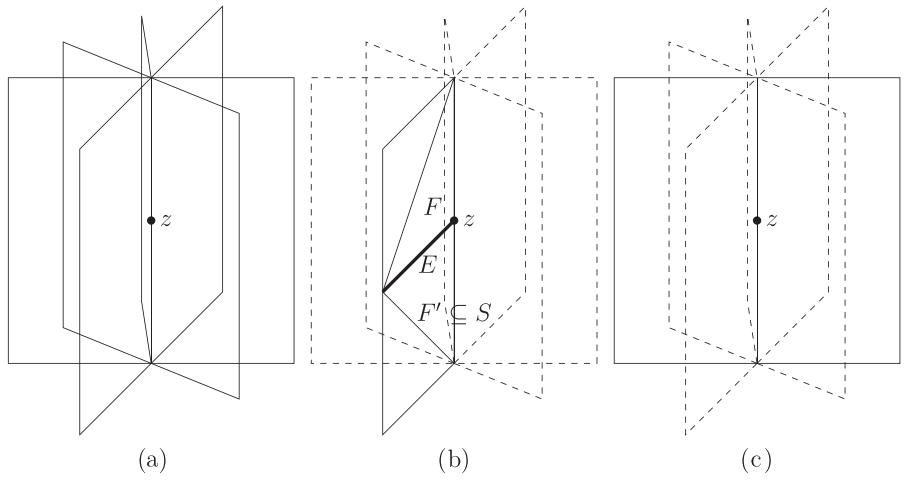

FIG. 4. Illustration of vertical hyperplanes in the proof of the inf–sup condition.

Since $v_F(3) \neq 0$, this implies

$$q|_{T_+} = q|_{T_-}.$$

It follows that q can jump across vertical faces only, i.e., if $v_F(3) = 0$; see Fig. 4a for a possible configuration of vertical hyperplanes where q can jump.

Now let F be a vertical face. We now have to treat the two different possible choices of ansatz spaces separately.

Case 1: $V_{h,D} = V_{2,D}$. Let $E \subseteq F$ be an edge of $\mathcal{M}$ that satisfies the following conditions:

- $v_F|_E(2) \neq 0$;
- E is an interior edge of $\Omega_{\mathcal{M}}$ in the sense that $\mathrm{int}(E) \subseteq \Omega_{\mathcal{M}}$ for the relative interior $\mathrm{int}(E)$ of E (i.e., E without its endpoints);
- E is not vertical, i.e., $|x - z| \neq |(x - z)(3)|$ for all $x \in E \setminus \{z\}$.

See Fig. 4b for an illustration of a possible configuration. Define a function $v \in V_{0,\mathcal{M}}$ by $v = (0, v_2, 0)$ with

$$\begin{aligned} &v_2(\mathrm{mid}(E)) = 1, \\ &v_2(\mathrm{mid}(E')) = 0 \text{ for all edges } E' \text{ of } \mathcal{M} \text{ with } E \neq E' \\ &\quad \text{and } v_2(\tilde{z}) = 0 \text{ for all nodes } \tilde{z} \text{ of } \mathcal{M}. \end{aligned} \tag{3.2}$$

Define

$$S := \bigcup \{F' \mid E \subseteq F' \text{and } F' \text{is an interior face of } \mathcal{M} \text{ and } v_{F'}(3) = 0\}.$$

Since $q \in N_{\mathcal{M}}$ can jump across vertical faces only, an integration by parts proves

$$0 = \int_{\Omega_{\mathcal{M}}} q \operatorname{div}_h v \, \mathrm{d}x = \int_{\Omega_{\mathcal{M}}} q \frac{\partial v_2}{\partial x_2} \, \mathrm{d}x = \int_S [q]_S v_2 \nu_S(2) \, \mathrm{d}s = \nu_S(2) \, [q]_S \int_S v_2 \, \mathrm{d}s.$$

Since $\int_S v_2 \, \mathrm{d}s = \operatorname{area}(S)/12 \neq 0$, this implies that q is continuous at F. Therefore, it can jump at vertical faces with $|\nu_F(1)| = 1$ only (otherwise there exists an edge E that satisfies the above conditions). Figure 4c illustrates a vertical hyperplane with $|\nu_F(1)| = 1$.

Case 2: $V_{h,D} = V_{\mathcal{F},D}$. In this case, define a function $v \in V_{0,\mathcal{M}}$ by $v = (0, v_2, 0)$ with

$$v_2 = \varphi_F. \tag{3.3}$$

Then $v_2|_{F'} = 0$ for all faces $F' \in \mathcal{F}$ with $F' \neq F$. Since $q \in N_{\mathcal{M}}$ can jump across vertical faces only, an integration by parts proves

$$0 = \int_{\Omega_{\mathcal{M}}} q \operatorname{div}_h v \, \mathrm{d}x = \int_{\Omega_{\mathcal{M}}} q \frac{\partial v_2}{\partial x_2} \, \mathrm{d}x = \int_F [q]_F v_2 \nu_F(2) \, \mathrm{d}s = \nu_F(2) [q]_F \int_F v_2 \, \mathrm{d}s.$$

Since $\int_F v_2 \, \mathrm{d}s = \operatorname{area}(F) \neq 0$, this implies that q is continuous at F whenever $\nu_F(2) \neq 0$.

In both cases, the only situation where q can jump is at vertical faces with $|\nu_F(1)| = 1$; see Fig. 4c for an illustration. Define $v = (v_1, 0, 0) \in V_{0,\mathcal{M}}$ by $v_1(z) = 1$ and let

$$S := \bigcup \left\{ F' \mid F' \text{ is an interior face of } \mathcal{M} \text{ and } \nu_F(1) = 1 \right\}.$$

Since q can jump across S only, an integration by parts then proves

$$0 = \int_{\Omega_{\mathcal{M}}} q \operatorname{div}_h v \, \mathrm{d}x = \int_{\Omega_{\mathcal{M}}} q \frac{\partial v_1}{\partial x_1} \, \mathrm{d}x = \int_S [q]_S v_1 \nu_S(1) \, \mathrm{d}s = [q]_S \int_S v_1 \, \mathrm{d}s.$$

Since $\int_S v_1 \, \mathrm{d}s = \operatorname{area}(S)/3 \neq 0$, this implies that q is continuous on $\Omega_{\mathcal{M}}$.

Let $\mathcal{F}(z) := \{F \in \mathcal{F} \mid z \in F\}$ denote the set of faces that shares the vertex z. The above argument proves that the two seminorms

$$\rho_1(p_h) := \sqrt{\sum_{F \in \mathcal{F}(z)} h_F \|[p_h]_F\|_{0,F}^2},$$

$$\rho_2(p_h) := \sup_{v_h \in V_{0,\mathcal{M}} \setminus \{0\}} \frac{\int_{\omega_z} p_h \operatorname{div}_h v_h \, \mathrm{d}x}{\|\nabla_h v\|_0}$$

are equivalent on $Q_{\mathcal{M}}$. A scaling argument proves that the constant is independent of the mesh size. This proves a local inf–sup condition with respect to the (semi)norm ρ_1. Assumption 3.4 guarantees that the

domain can be covered by the macroelements $\mathcal{M}$. Then Stenberg (1990, Lemmas 1–4) proves the global inf–sup condition

$$\|p_h\|_0 \lesssim \sup_{v\in V_{h,D}\setminus\{0\}} \frac{b_h(v_h,p_h)}{\|\nabla_h v_h\|_0}$$

with p_h measured in the L^2 norm.

Step 2. Let $(u_h,p_h)\in V_{h,D}\times Q_h$ be given and define for abbreviation

$$B := \sup_{(v_h,q_h)\in(V_{h,D}\times Q_h)\setminus\{0\}} \frac{\mathcal{B}(u_h,p_h;v_h,q_h)}{|\!|\!|(v_h,q_h)|\!|\!|_h}.$$

Step 1 guarantees the existence of $v_h\in V_{h,D}$ with $\|\nabla_h v_h\|_{L^2(\Omega)}=1$ and

$$\|p_h\|_0 \lesssim b_h(v_h,p_h) = \mathcal{B}(u_h,p_h;v_h,0) - a_h(u_h,v_h) \le B + \|\nabla_h u_h\|_0,$$

which implies

$$|\!|\!|(u_h,p_h)|\!|\!|_h^2 \lesssim B^2 + \|\nabla_h u_h\|_0^2.$$

The discrete Korn inequality from Theorem 3.9 implies

$$\|\nabla_h u_h\|_0 \lesssim \|\varepsilon_h(u_h)\|_0.$$

This implies

$$\|\nabla_h u_h\|_0^2 \lesssim \|\varepsilon_h(u_h)\|_0^2 = \mathcal{B}(u_h,0;u_h,0) \le B\,|\!|\!|(u_h,p_h)|\!|\!|_h,$$

and therefore

$$|\!|\!|(u_h,p_h)|\!|\!|_h \lesssim B.$$

This concludes the proof. □

REMARK 3.11 The proof of Theorem 3.10 does not work in the case $V_{h,D}=S_D^{\mathrm{C},1}\times S_D^{\mathrm{C},1}\times S_D^{\mathrm{NC},1}$: in this situation, the test functions v_2 that were defined in (3.2) and in (3.3) have only one degree of freedom and, therefore, only the linear combination

$$\sum_{F\in\mathcal{F}(\Omega_\mathcal{M}),\,F\text{ is vertical}} [q]_F v_F(2)\,\mathrm{area}(F) = 0$$

has to vanish, but the continuity on all F with $|v_F(2)|<1$ cannot be concluded.

From the discrete inf–sup condition from Theorem 3.10, the discrete Korn inequality from Theorem 3.9 and the standard theory in mixed FEMs (Boffi *et al.*, 2013), we can immediately show the well-posedness of the problem which is stated in the following corollary.

COROLLARY 3.12 Let $V_{h,D}=V_{2,D}$ or $V_{h,D}=V_{\mathcal{F},D}$. There exists a unique solution $(u_h,p_h)\in V_{h,D}\times Q_h$ to (2.1) and it satisfies

$$\|u_h\|_{1,h} + \|p_h\|_{L^2(\Omega)} \lesssim \|g\|_{L^2(\Omega)}.$$

Recently, a new approach in the error analysis of nonconforming FEMs was introduced (Gudi, 2010). This approach employs techniques from the *a posteriori* analysis to conclude *a priori* results. This leads to *a priori* error estimates that are independent of the regularity of the exact solution and that hold on arbitrary coarse meshes. This approach was generalized by Hu *et al.* (2014) to the case of nonconstant stresses. The stability results of Theorems 3.9 and 3.10 and the abstract *a posteriori* framework of Carstensen (2005) and Carstensen & Hu (2007) are the key ingredients in the following error estimate. The right-hand side of this error estimate includes oscillations of the right-hand side g, which are defined by

$$\operatorname{osc}(g, \mathcal{T}) := \|h_{\mathcal{T}}(g - \Pi_0 g)\|_{L^2(\Omega)},$$

where Π_0 denotes the L^2 projection to piecewise constant functions. If g is (piecewise) smooth, this term is of higher order.

THEOREM 3.13 (Best-approximation error estimate). Assume that Assumptions 3.1 and 3.4 hold. Let $(u, p) \in \left[H^1_D(\Omega)\right]^3 \times L^2(\Omega)$ be the exact solution of problem (2.2) and $(u_h, p_h) \in V_{h,D} \times Q_h$ be the discrete solution of (2.1) for $V_{h,D} = V_{2,D}$ or $V_{h,D} = V_{\mathcal{F},D}$. Then it holds that

$$\begin{aligned}\|u - u_h\|_{1,h} + \|p - p_h\|_{L^2(\Omega)} \\ \lesssim \inf_{v_h \in V_{h,D}} \|u - v_h\|_{1,h} + \inf_{q_h \in Q_h} \|p - q_h\|_{L^2(\Omega)} + \|\varepsilon(u) - \Pi_0 \varepsilon(u)\|_{L^2(\Omega)} + \operatorname{osc}(g, \mathcal{T}).\end{aligned}$$

Proof. The proof is in the spirit of Gudi (2010), Badia *et al.* (2014) and the generalization of Hu *et al.* (2014). The outline of the proof is included for completeness.

Let $(w_h, r_h) \in V_{h,D} \times Q_h$ be arbitrary. The inf–sup condition of Theorem 3.10 guarantees the existence of $(v_h, q_h) \in V_{h,D} \times Q_h$ with $|||(v_h, q_h)||| = 1$ and

$$\|u_h - w_h\|_{1,h} + \|p_h - r_h\|_{L^2(\Omega)} \lesssim \mathcal{B}(u_h - w_h, p_h - r_h; v_h, q_h).$$

Let $E_h : V_{h,D} \to \left[H^1_D(\Omega)\right]^3$ be the operator that is the identity in the first two components and an averaging (enriching) operator that maps $S^{\mathrm{NC},1}_D$ to $S^{\mathrm{C},1}_D$ in the third component; see the study by Gudi (2010) for details. As (u, p) is the exact solution and (u_h, p_h) is the discrete solution, this implies

$$\begin{aligned}\mathcal{B}(u_h - w_h, p_h - r_h; v_h, q_h) \\ = (g, v_h - E_h v_h)_{L^2(\Omega)} + \mathcal{B}(u - w_h, p - r_h; E_h v_h, q_h) - \mathcal{B}(w_h, r_h; v_h - E_h v_h, 0).\end{aligned}$$

A Cauchy inequality and the stability of the enriching operator E_h prove

$$|\mathcal{B}(u - w_h, p - r_h; E_h v_h, q_h)| \le \|u - w_h\|_{1,h} + \|p - r_h\|_{L^2(\Omega)}.$$

Let $\tau_h := 2\mu\varepsilon_h(w_h) - r_h I_{3\times 3}$ denote the stress-like variable for w_h and r_h. A piecewise integration by parts proves, for the remaining terms,

$$\begin{aligned}|(g, v_h - E_h v_h)_{L^2(\Omega)} + \mathcal{B}(w_h, r_h; v_h - E_h v_h, 0)| \\ = (g - \operatorname{div}_h \tau_h, v_h - E_h v_h)_{L^2(\Omega)} + \sum_{F\in\mathcal{F}} \int_F \big[(v_h - E_h v_h)\cdot \tau_h \nu_F\big]_F \,\mathrm{d}s.\end{aligned} \tag{3.4}$$

The first term on the right-hand side is estimated with the help of a Cauchy inequality and the approximation properties of E_h (Gudi, 2010):

$$(g - \operatorname{div}_h \tau_h, v_h - E_h v_h)_{L^2(\Omega)} \lesssim \|h_{\mathcal{T}}(g - \operatorname{div}_h \tau_h)\|_{L^2(\Omega)}.$$

This is a standard *a posteriori* error estimator term (Carstensen, 2005; Carstensen & Hu, 2007) and the bubble function technique (Verfürth, 2013) proves the efficiency

$$\|h_{\mathcal{T}}(g - \operatorname{div}_h \tau_h)\|_{L^2(\Omega)} \lesssim \|u - w_h\|_{1,h} + \|p - r_h\|_{L^2(\Omega)} + \operatorname{osc}(g, \mathcal{T}).$$

Let $\langle\bullet\rangle_F := (\bullet|_{T_+} + \bullet|_{T_-})/2$ denote the average along $F = T_+ \cap T_-$. An elementary calculation proves for any α and β that $[\alpha\beta_F] = \langle\alpha\rangle_F[\beta]_F + [\alpha]_F\langle\beta\rangle_F$. We employ this identity for the second term of the right-hand side of (3.4) and conclude

$$\int_F \big[(v_h - E_h v_h)\cdot \tau_h \nu_F\big]_F \,\mathrm{d}s = \int_F [v_h - E_h v_h]_F \cdot \langle \tau_h \nu_F\rangle_F \,\mathrm{d}s + \int_F \langle v_h - E_h v_h\rangle_F \cdot [\tau_h \nu_F]_F \,\mathrm{d}s.$$

The second term on the right-hand side is again estimated with *a posteriori* techniques (Carstensen, 2005; Carstensen & Hu, 2007; Verfürth, 2013) which results in

$$\begin{aligned}\sum_{F\in\mathcal{F}} \int_F \langle v_h - E_h v_h\rangle_F \cdot [\tau_h \nu_F]_F \,\mathrm{d}s &\lesssim \left(\sum_{F\in\mathcal{F}} h_F \|[\tau_h]_F \nu_F\|^2_{L^2(F)}\right)^{1/2} \\ &\lesssim \|u - w_h\|_{1,h} + \|p - r_h\|_{L^2(\Omega)} + \operatorname{osc}(g, \mathcal{T}).\end{aligned}$$

Since $[v_h - E_h v_h]_F$ is affine on $F = T_+ \cap T_-$ and vanishes at the midpoint of F, we conclude for the first term, as in the study by Hu *et al.* (2014), that

$$\begin{aligned}\int_F [v_h - E_h v_h]_F \cdot \langle \tau_h \nu_F\rangle_F \,\mathrm{d}s &= \int_F [v_h - E_h v_h]_F \cdot \langle (1 - \Pi_0)\tau_h \nu_F\rangle_F \,\mathrm{d}s \\ &= \frac{1}{2}\int_F [v_h - E_h v_h]_F \cdot ((1 - \Pi_0)\tau_h|_{T_+} + (1 - \Pi_0)\tau_h|_{T_-})\nu_F \,\mathrm{d}s.\end{aligned}$$

Note that $\tau_h = 2\mu\varepsilon_h(w_h) - r_h I_{3\times 3}$ and r_h is piecewise constant. Therefore, trace inequalities (Brenner & Scott, 2008) and an inverse inequality imply that this is bounded by

$$\begin{aligned}\frac{1}{2}\int_F [v_h - E_h v_h]_F \cdot ((1-\Pi_0)\tau_h|_{T_+} + (1-\Pi_0)\tau_h|_{T_-})\nu_F \,\mathrm{d}s \\ &\lesssim \|(1-\Pi_0)\tau_h\|_{L^2(T_+\cup T_-)} \\ &\le \|(1-\Pi_0)\varepsilon_h(u-w_h)\|_{L^2(T_+\cup T_-)} + \|(1-\Pi_0)\varepsilon(u)\|_{L^2(T_+\cup T_-)}.\end{aligned}$$

Since $\|(1-\Pi_0)\varepsilon_h(u-w_h)\|_{L^2(T_+\cup T_-)} \le \|\varepsilon_h(u-w_h)\|_{L^2(T_+\cup T_-)}$, the combination of the foregoing inequalities and the finite overlap of the patches conclude the proof. □

4. Counterexamples for P_1–P_0 discretization

The following two counterexamples prove that the inf–sup condition for the ansatz space $S_D^{\mathrm{C},1} \times S_D^{\mathrm{C},1} \times S_D^{\mathrm{NC},1}$ cannot hold in general, as well as that a discrete Korn inequality for the ansatz space $S_D^{\mathrm{C},1} \times S_D^{\mathrm{NC},1} \times S_D^{\mathrm{NC},1}$ is not satisfied in general.

4.1 *Instability of* $S_D^{\mathrm{C},1} \times S_D^{\mathrm{C},1} \times S_D^{\mathrm{NC},1}$

The following counterexample proves that the inf–sup condition

$$\|p_h\|_0 \lesssim \sup_{v_h \in V_{h,D}\setminus\{0\}} \frac{b_h(v_h, p_h)}{\|\nabla_h v_h\|_0} \qquad \text{for all } p_h \in Q_h \tag{4.1}$$

is not fulfilled for functions in $S_D^{\mathrm{C},1} \times S_D^{\mathrm{C},1} \times S_D^{\mathrm{NC},1}$.

Consider the node $z := (0,0,0)$ with nodal patch

$$\begin{aligned}\mathcal{T} &:= \left\{ T_{jk\ell} \mid (j,k,\ell) \in \{1,2\}^3 \right\} \\ \text{with} \quad T_{jk\ell} &:= \operatorname{conv}\left\{ z, (-1)^j e_1, (-1)^k e_2, (-1)^\ell e_3 \right\}\end{aligned} \tag{4.2}$$

with the unit vectors e_1, e_2 and e_3; see Fig. 5 for an illustration. Let $\Omega := \bigcup \mathcal{T}$ be the corresponding domain with pure Dirichlet boundary $\Gamma_D = \partial\Omega$. Define the function $q \in P_0(\mathcal{T})$ by

$$\begin{aligned}\tilde{q}|_{T_{111}} := \tilde{q}|_{T_{112}} := 1, \qquad \tilde{q}|_{T_{121}} := \tilde{q}|_{T_{122}} := 0, \\ \tilde{q}|_{T_{211}} := \tilde{q}|_{T_{212}} := 0, \qquad \tilde{q}|_{T_{221}} := \tilde{q}|_{T_{222}} := 1\end{aligned}$$

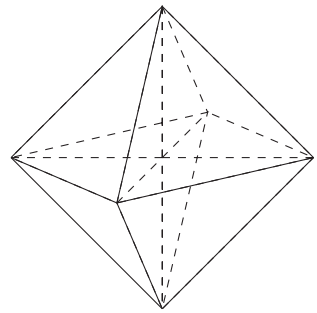

FIG. 5. Triangulation of Sections 4.1 and 4.2.

and $q = \tilde{q} - \int_\Omega \tilde{q}\,\mathrm{d}x$. The normal vectors to the following intersections are written

$$\begin{aligned}
&\text{for } E_1 := (T_{111} \cup T_{112}) \cap (T_{121} \cup T_{122}) \text{ define } \nu_1 = (0,1,0),\\
&\text{for } E_2 := (T_{111} \cup T_{112}) \cap (T_{211} \cup T_{212}) \text{ define } \nu_2 = (1,0,0),\\
&\text{for } E_3 := (T_{221} \cup T_{222}) \cap (T_{121} \cup T_{122}) \text{ define } \nu_2 = (1,0,0),\\
&\text{for } E_4 := (T_{221} \cup T_{222}) \cap (T_{211} \cup T_{212}) \text{ define } \nu_2 = (0,1,0).
\end{aligned}$$

Let $v_h = (v_1, v_2, v_3) \in S_D^{\mathrm{C},1} \times S_D^{\mathrm{C},1} \times S_D^{\mathrm{NC},1}$. Since v_1 and v_2 have only one degree of freedom, it follows that $v_1(\mathrm{mid}(F)) = v_1(\mathrm{mid}(F'))$ for all faces F, F'. An integration by parts then proves

$$\int_{\Omega_z} q\frac{\partial v_1}{\partial x_1}\,\mathrm{d}x = \int_{E_2} [q]_{E_2} v_1\,\mathrm{d}s + \int_{E_3} [q]_{E_3} v_1\,\mathrm{d}s = 2v_1(\mathrm{mid}(F))([q]_{E_2} + [q]_{E_3}) = 0$$

and similarly

$$\int_{\Omega_z} q\frac{\partial v_2}{\partial x_2}\,\mathrm{d}x = 0.$$

Since the third components of all of the normal vectors for faces, where q jumps, vanish, a further integration by parts leads to

$$\int_{\Omega_z} q\frac{\partial v_3}{\partial x_3}\,\mathrm{d}x = 0.$$

The sum of the last three equalities yields

$$\int_{\Omega_z} q\,\mathrm{div}\, v_h\,\mathrm{d}x = 0.$$

Since $v_h \in V_{h,D}$ is arbitrary, this proves that the inf–sup condition (4.1) cannot hold, and, hence, a discretization with the space $S_D^{\mathrm{C},1} \times S_D^{\mathrm{C},1} \times S_D^{\mathrm{NC},1}$ is not stable.

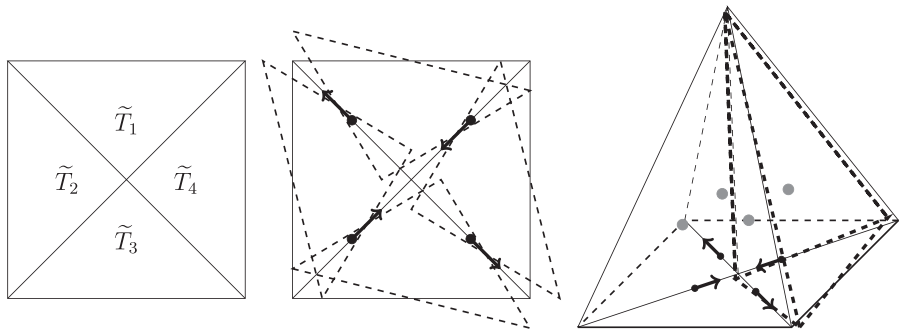

(a) Two-dimensional triangulation (b) Two-dimensional counterexample (c) Generalization to three dimensions

FIG. 6. Generalization of two-dimensional counterexample for the instability of $S_D^{\mathrm{C},1} \times S_D^{\mathrm{NC},1} \times S_D^{\mathrm{NC},1}$.

4.2 *Instability of* $S_D^{\mathrm{C},1} \times S_D^{NC,1} \times S_D^{NC,1}$

The following counterexamples prove that there are functions in $S_D^{\mathrm{C},1} \times S_D^{\mathrm{NC},1} \times S_D^{\mathrm{NC},1}$ such that $\varepsilon_h(\bullet)$ vanishes, but which are not global rigid body motions. This proves that a Korn inequality cannot hold on $S_D^{\mathrm{C},1} \times S_D^{\mathrm{NC},1} \times S_D^{\mathrm{NC},1}$. The first part illustrates how a missing Korn inequality for the discretization $S_D^{\mathrm{NC},1} \times S_D^{\mathrm{NC},1}$ in the two-dimensional situation generalizes to the three-dimensional case, while the second part proves that there exist arbitrarily fine meshes, such that a counterexample can be constructed.

For the first counterexample, consider first the two-dimensional square $\widetilde{\Omega} = (-1, 1)^2$ with the two-dimensional triangulation $\mathcal{T}_{2D} = \{\widetilde{T}_1, \widetilde{T}_2, \widetilde{T}_3, \widetilde{T}_4\}$ with triangles $\widetilde{T}_j$ as in Fig. 6a. Then a piecewise rigid body motion $\mathrm{RM}_{2\mathrm{D}}$ that is continuous at the midpoints of the (two-dimensional) edges of the triangulation is depicted in Fig. 6b. This counterexample is also given in the studies by Falk & Morley (1990, Sect. 5) and Arnold (1993) to prove that there are two-dimensional triangulations where Korn's inequality does not hold, even if boundary conditions are imposed. Consider now the triangulation $\mathcal{T} := \{T_1, T_2, T_3, T_4\}$ in three dimensions with $T_j := \mathrm{conv}\{(1, 0, 0), \widetilde{T}_j\}$, where $\widetilde{T}_j$ from above is considered as a set in the plane $\{0\} \times \mathbb{R}^2$. Shifting the continuity points of $\mathrm{RM}_{2\mathrm{D}}$, such that the function is continuous at $(-1/3, -1/3)$, $(-1/3, 1/3)$, $(1/3, -1/3)$, $(1/3, 1/3)$, a piecewise rigid body motion with respect to $\mathcal{T}$ is given by $\mathrm{RM}_{3\mathrm{D}}(x) := (0, \mathrm{RM}_{2\mathrm{D}}(x_2, x_3))$. Since it is continuous at the points $(0, -1/3, -1/3)$, $(0, -1/3, 1/3)$, $(0, 1/3, -1/3)$, $(0, 1/3, 1/3)$ and constant in the x-direction, it is also continuous at the midpoints of the interior faces. This proves that a Korn inequality cannot hold for the space $S_D^{\mathrm{C},1} \times S_D^{\mathrm{NC},1} \times S_D^{\mathrm{NC},1}$.

For the second part, let the triangulation $\widehat{\mathcal{T}}$ be given by $\widehat{\mathcal{T}} := \{\widehat{T}_1, \widehat{T}_2, \widehat{T}_3, \widehat{T}_4\}$ with the tetrahedra

$$\widehat{T}_1 := \mathrm{conv}\{(0,0,0), (1,0,0), (0,1,0), (0,0,1)\},$$
$$\widehat{T}_2 := \mathrm{conv}\{(0,0,0), (1,0,0), (0,-1,0), (0,0,1)\},$$
$$\widehat{T}_3 := \mathrm{conv}\{(0,0,0), (1,0,0), (0,-1,0), (0,0,-1)\},$$
$$\widehat{T}_4 := \mathrm{conv}\{(0,0,0), (1,0,0), (0,1,0), (0,0,-1)\};$$

TABLE 1 *Number of degrees of freedom in the numerical experiments in Sections 5.1–5.4*

Level of refinement	Cube			L-shaped domain		
	KS bubbles	KS P_2	BR	KS bubbles	KS P_2	BR
1	1.7e+02	1.3e+02	1.0e+02	5.1e+02	3.9e+02	3.2e+02
2	1.5e+03	1.2e+03	9.7e+02	4.5e+03	3.6e+03	2.9e+03
3	1.2e+04	1.0e+04	8.3e+03	3.8e+04	3.1e+04	2.5e+04
4	1.0e+05	8.8e+04	6.9e+04	3.1e+05	2.6e+05	2.0e+05
5	8.6e+05	7.2e+05	5.6e+05			

see Fig. 7 for an illustration. Let $a \in \mathbb{R}$ be arbitrary. Define a piecewise rigid body motion φ by

$$\varphi_{\widehat{T}_1}(x) := (0, a - 3ax_3, -a + 3ax_2),$$
$$\varphi_{\widehat{T}_4}(x) := (0, -a + 3ax_3, -a - 3ax_2),$$
$$\varphi_{\widehat{T}_4}(x) := (0, -a - 3ax_3, a + 3ax_2),$$
$$\varphi_{\widehat{T}_4}(x) := (0, a + 3ax_3, a - 3ax_2).$$

This function is continuous at the interior face's midpoints and vanishes at the midpoints of the boundary faces. Therefore it can be extended by zero to the rectangle $(0, 1) \times (-1, 1) \times (-1, 1)$. As those functions can be easily glued together, this proves that even for arbitrarily fine mesh sizes, there exist piecewise rigid body motions in $S_D^{\mathrm{C},1} \times S_D^{\mathrm{NC},1} \times S_D^{\mathrm{NC},1}$.

5. Numerical experiments

This section compares the performances of the two suggested discretizations from Section 2 and the conforming Bernardi–Raugel FEM in numerical experiments. The Bernardi–Raugel FEM (Bernardi & Raugel, 1985) is a conforming FEM that approximates the velocity in the space

$$V_{\mathrm{BR}} := \left\{ v_h \in (H_D^1(\Omega))^3 \;\middle|\; \begin{array}{l} \exists\, v_{\mathrm{C}} \in (S^{\mathrm{C},1})^3 \text{ and } \forall\, F \in \mathcal{F},\ \exists\, \alpha_F \in \mathbb{R} \text{ such that} \\ v_h = v_{\mathrm{C}} + \sum_{F \in \mathcal{F} \setminus \mathcal{F}(\Gamma_D)} \alpha_F \varphi_F \nu_F \end{array} \right\},$$

where ν_F denotes the normal for a face F and φ_F denotes the face bubble defined in Section 2. The pressure is approximated in Q_h. The errors of the different methods are compared in the following subsections, while the computational effort of the three different methods is illustrated in Tables 1–2 in terms of the number of nonzero entries of the system matrices and the number of degrees of freedom. The number of degrees of freedom is lower for the Bernardi–Raugel method compared to the two proposed methods. However, since the support of the face bubble functions in $V_{\mathcal{F},D}$ consists of only two tetrahedra, the numbers of nonzero entries of the system matrices of the Bernardi–Raugel FEM and the proposed FEM with $V_{h,D} = V_{\mathcal{F},D}$ show only slight differences.

TABLE 2 *Number of nonzero entries in the system matrix in the numerical experiments in Sections 5.1–5.4*

Level of refinement	Cube			L-shaped domain		
	KS bubbles	KS P_2	BR	KS bubbles	KS P_2	BR
1	5.4e+03	6.2e+03	5.3e+03	1.5e+04	1.7e+04	1.5e+04
2	4.0e+04	4.4e+04	3.9e+04	1.1e+05	1.3e+05	1.1e+05
3	3.1e+05	3.4e+05	3.0e+05	9.3e+05	1.0e+06	8.9e+05
4	2.4e+06	2.7e+06	2.3e+06	7.4e+06	8.0e+06	7.0e+06
5	1.9e+07	2.1e+07	1.8e+07			

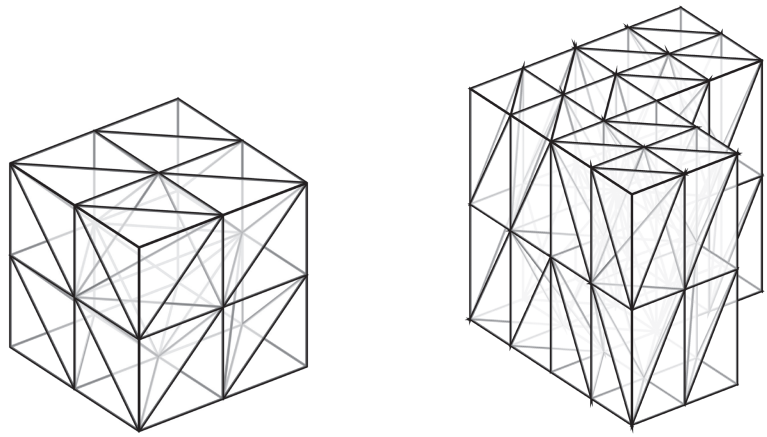

FIG. 8. Initial triangulations of the cube and the tensor product L-shaped domain.

5.1 *Smooth solution on the cube, I*

This subsection considers the smooth solution

$$u(x) = \begin{pmatrix} \pi \cos(\pi x_2) \sin(\pi x_1)^2 \sin(\pi x_2) \sin(\pi x_3) \\ -\pi \cos(\pi x_1) \sin(\pi x_2)^2 \sin(\pi x_1) \sin(\pi x_3) \\ 0 \end{pmatrix},$$
$$p(x) = 0$$

on the cube $\Omega = (0,1)^3$ with Neumann boundary $\Gamma_N = (0,1)^2 \times \{0\}$ and Dirichlet boundary $\Gamma_D = \partial\Omega \setminus \Gamma_N$. The solutions to (2.1) with $V_{h,D} = V_{2,D}$ and $V_{h,D} = V_{\mathcal{F},D}$ and the solution for the Bernardi–Raugel (BR) FEM for the right-hand side f and g given by the exact solution are computed on a sequence of red-refined triangulations. The initial triangulation is depicted in Fig. 8. The H^1 errors and the L^2 errors of the velocity u are depicted in the convergence history plot in Fig. 9. The H^1 errors show convergence rates of $\mathcal{O}(h)$ for all methods, while the convergence rates of the L^2 errors of all methods are near $\mathcal{O}\left(h^2\right)$ with a slightly larger convergence rate for $V_{2,D}$.

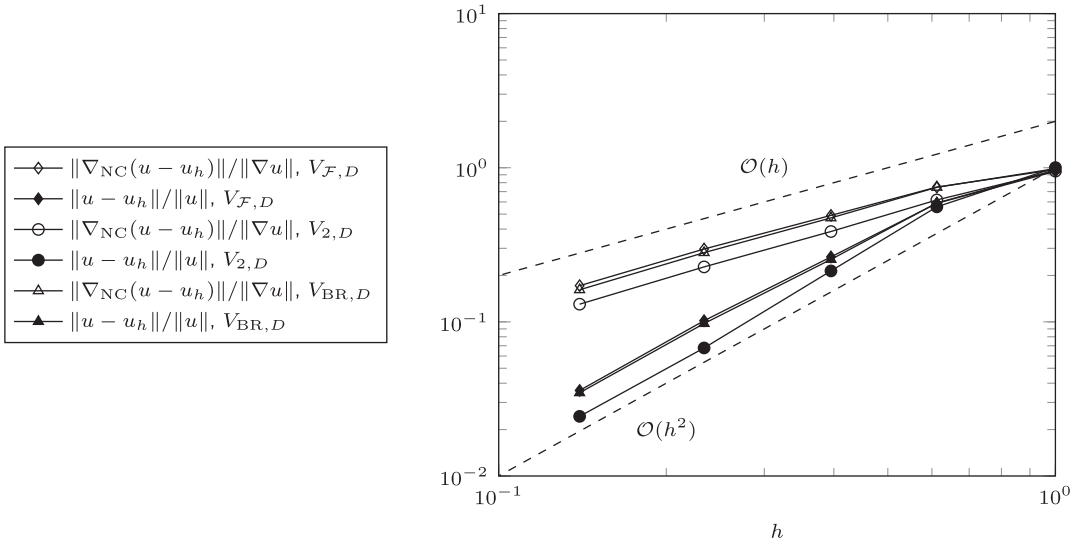

FIG. 9. Convergence history plot for the example from Section 5.1.

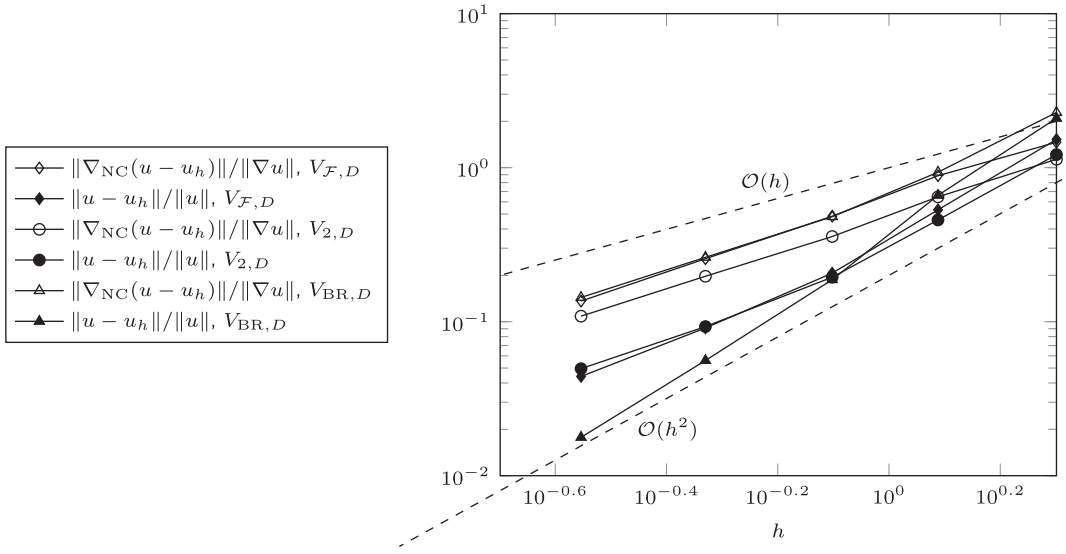

FIG. 10. Convergence history plot for the example from Section 5.2.

5.2 *Smooth solution on the cube, II*

This subsection considers the smooth exact solution

$$u(x) = \begin{pmatrix} 10x_1x_2^4 + 10x_1x_3^4 - 4x_1^5 \\ 10x_2x_1^4 + 10x_2x_3^4 - 4x_2^5 \\ 10x_3x_1^4 + 10x_3x_2^4 - 4x_3^5 \end{pmatrix},$$
$$p(x) = -60x_1^2x_2^2 - 60x_1^2x_3^2 - 60x_2^2x_3^2 + 20x_1^4 + 20x_2^4 + 20x_3^4$$

on the cube $\Omega = (-1,1)^3$ with Neumann boundary $\Gamma_N = (0,1)^2 \times \{-1\}$ and Dirichlet boundary $\Gamma_D = \partial\Omega \setminus \Gamma_N$. As in Section 5.1, the solutions to (2.1) with $V_{h,D} = V_{2,D}$ and $V_{h,D} = V_{\mathcal{F},D}$ and the solution of the Bernardi–Raugel FEM for the right-hand side f and g given by the exact solution are computed on a sequence of red-refined triangulations. The initial triangulation is depicted in Fig. 8. The H^1 errors and the L^2 errors of the velocity u are depicted in the convergence history plot in Fig. 10. The H^1 errors show convergence rates of $\mathcal{O}(h)$ for all methods, while the convergence rates of the L^2 errors of both nonconforming methods are slightly worse than $\mathcal{O}\left(h^2\right)$. The convergence rate of the L^2 error for the Bernardi–Raugel FEM seems to be larger than that of the two nonconforming FEMs.

5.3 *Smooth solution on the cube, III*

This subsection considers the smooth exact solution

$$u(x) = \begin{pmatrix} 2x_2x_3(x_1^2-1)^2(x_2^2-1)(x_3^2-1) \\ -x_1x_3(x_1^2-1)(x_2^2-1)^2(x_3^2-1) \\ -x_1x_2(x_1^2-1)(x_2^2-1)(x_3^2-1)^2 \end{pmatrix},$$
$$p(x) = x_1x_2x_3$$

on the cube $\Omega = (-1,1)^3$ with Neumann boundary $\Gamma_N = (0,1)^2 \times \{-1\}$ and Dirichlet boundary $\Gamma_D = \partial\Omega \setminus \Gamma_N$. As in Sections 5.1–5.2, the solutions to (2.1) with $V_{h,D} = V_{2,D}$ and $V_{h,D} = V_{\mathcal{F},D}$ and the solution of the Bernardi–Raugel FEM for the right-hand side f and g given by the exact solution are computed on a sequence of red-refined triangulations. The initial triangulation is depicted in Fig. 8. The H^1 errors and the L^2 errors of the velocity u are depicted in the convergence history plot in Fig. 11. The H^1 errors show convergence rates slightly worse than $\mathcal{O}(h)$ for all three methods. As the convergence rate still increases under the considered refinements, it is suggested that the asymptotic regime is not reached at this point. The convergence rates of the L^2 errors of all three methods are $\mathcal{O}\left(h^2\right)$ for all methods.

5.4 *Singular solution on the three-dimensional tensor product L-shaped domain*

This subsection considers the tensor product L-shaped domain

$$\Omega = \Big((-1,1)^2 \setminus ([0,1] \times [-1,0])\Big) \times (-1,1)$$

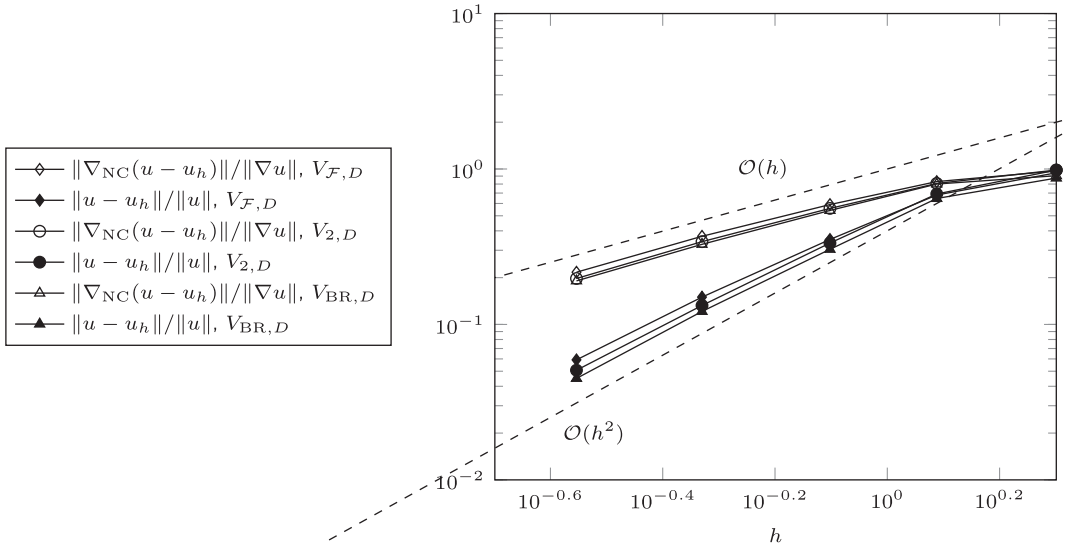

FIG. 11. Convergence history plot for the example from Section 5.3.

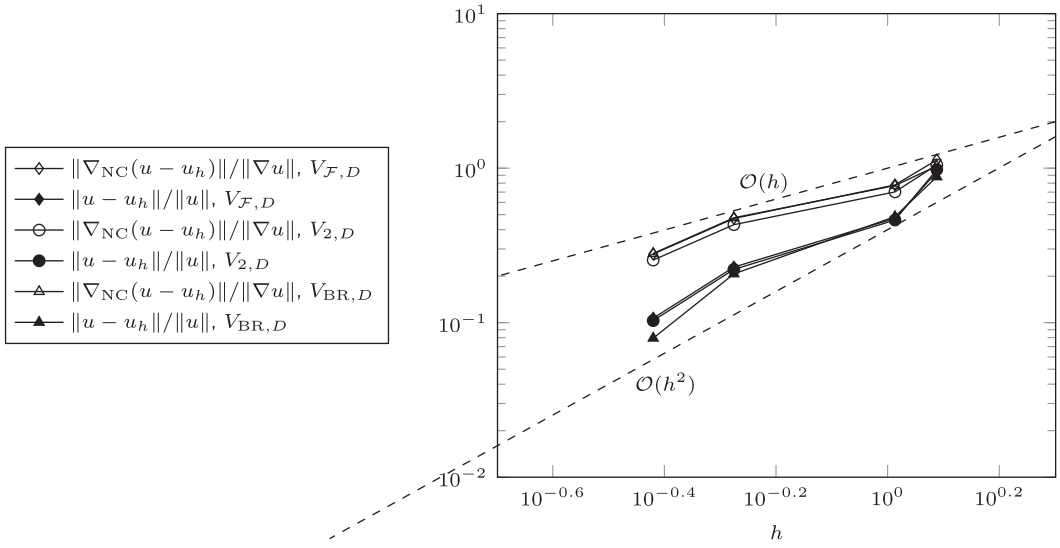

FIG. 12. Convergence history plot for the example from Section 5.4.

with $\Gamma_N := \{1\} \times (0,1) \times (-1,1)$ and exact solution

$$u(x_1,x_2,x_3) = \operatorname{curl} \begin{pmatrix} (1-x_3^2)^2 u_{\mathrm{Gr}}(x_1,x_2) \\ \cos(\pi x_3) u_{\mathrm{Gr}}(x_1,x_2) \\ x_3 u_{\mathrm{Gr}}(x_1,x_2), \end{pmatrix} \quad \text{and} \quad p = 0,$$

where u_{Gr} is the singular solution for the two-dimensional plate problem on the L-shaped domain from Grisvard (1992, p. 107) and in polar coordinates is written

$$u_{\mathrm{Gr}}(r,\theta) = \left(r^2\cos^2\theta - 1\right)^2 \left(r^2 \sin^2\theta - 1\right)^2 r^{1+\alpha}\, g(\theta).$$

Here $\alpha := 0.544483736782464$ is a noncharacteristic root of $\sin^2(\alpha\omega) = \alpha^2 \sin^2(\omega)$ for $\omega := 3\pi/2$ and

$$\begin{aligned} g(\theta) = &\left[\frac{\sin((\alpha-1)\omega)}{\alpha-1} - \frac{\sin((\alpha+1)\omega)}{\alpha+1}\right](\cos((\alpha-1)\theta) - \cos((\alpha+1)\theta)) \\ &- \left[\frac{\sin((\alpha-1)\theta)}{\alpha-1} - \frac{\sin((\alpha+1)\theta)}{\alpha+1}\right](\cos((\alpha-1)\omega) - \cos((\alpha+1)\omega)). \end{aligned}$$

The right-hand side data f and g are chosen according to the exact solution. The initial triangulation is depicted in Fig. 8. The H^1 and L^2 errors are plotted in Fig. 12 against the mesh size. Although the exact solution is not in $H^2(\Omega)$, the convergence rate of the H^1 errors for all three methods seems to be $\mathcal{O}(h)$, at least in a pre-asymptotic regime. This is in agreement with numerical experiments in two dimensions and three dimensions for the plate problem, where the reduced convergence rate can be seen only in the regime of very fine meshes. The L^2 errors show convergence rates slightly smaller than $\mathcal{O}\left(h^2\right)$ for the three considered methods, but the Bernardi–Raugel FEM seems to have a slightly better convergence rate than the two nonconforming FEMs.

Acknowledgements

Parts of this article were written while the second author enjoyed the kind hospitality of the Hausdorff Institute for Mathematics (Bonn, Germany). Both authors would like to thank the supports of the fifth and sixth Chinese–German workshops on Applied and Computational Mathematics held at the University of Augsburg, Germany, from September 21st to 25th, 2015 and the Tongji University, China, from October 9th to 13th, 2017.

Funding

NSFC Project (11625101 to J.H.); DFG Priority Program 1748 under the project 'Robust and Efficient Finite Element Discretizations for Higher-Order Gradient Formulations' (SCHE1885/1-1 to M.S.)

References

Arnold, D. N. (1993) On nonconforming linear-constant elements for some variants of the Stokes equations. *Istit. Lombardo Accad. Sci. Lett. Rend A*, **127**, 83–93.

Badia, S., Codina, R., Gudi, T. & Guzmán, J. (2014) Error analysis of discontinuous Galerkin methods for the Stokes problem under minimal regularity. *IMA J. Numer. Anal.*, **34**, 800–819.

Bernardi, C. & Raugel, G. (1985) Analysis of some finite elements for the Stokes problem. *Math. Comp.*, **44**, 71–79.

Boffi, D. (1997) Three-dimensional finite element methods for the Stokes problem. *SIAM J. Numer. Anal.*, **34**, 664–670.

Boffi, D., Brezzi, F. & Fortin, M. (2013) *Mixed Finite Element Methods and Applications*. Springer Series in Computational Mathematics, vol. 44. Heidelberg: Springer.

Boffi, D., Cavallini, N., Gardini, F. & Gastaldi, L. (2012a) Local mass conservation of Stokes finite elements. *J. Sci. Comput.*, **52**, 383–400.

Boffi, D., Cavallini, N., Gardini, F. & Gastaldi, L. (2012b) Stabilized Stokes elements and local mass conservation. *Boll. Unione Mat. Ital.*, **5**, 543–573.

Brenner, S. C. (2003) Poincaré-Friedrichs inequalities for piecewise H^1 functions. *SIAM J. Numer. Anal.*, **41**, 306–324.

Brenner, S. C. (2004) Korn's inequalities for piecewise H^1 vector fields. *Math. Comp.*, **73**, 1067–1087.

Brenner, S. C. & Scott, L. R. (2008) *The Mathematical Theory of Finite Element Methods*, 3rd edn. Texts in Applied Mathematics, vol. 15. New York, Berlin, Heidelberg: Springer.

Carstensen, C. (2005) A unifying theory of a posteriori finite element error control. *Numer. Math.*, **100**, 617–637.

Carstensen, C. & Hu, J. (2007) A unifying theory of a posteriori error control for nonconforming finite element methods. *Numer. Math.*, **107**, 473–502.

Carstensen, C., Köhler, K., Peterseim, D. & Schedensack, M. (2015) Comparison results for the Stokes equations. *Appl. Numer. Math.*, **95**, 118–129. Published online.

Carstensen, C. & Schedensack, M. (2015) Medius analysis and comparison results for first-order finite element methods in linear elasticity. *IMA J. Numer. Anal.*, **35**, 1591–1621.

Crouzeix, M. & Raviart, P.-A. (1973) Conforming and nonconforming finite element methods for solving the stationary Stokes equations. I. *Rev. Française Automat. Informat. Recherche Opérationnelle Sér. Rouge*, **7**, 33–75 (R-3).

Falk, R. S. & Morley, M. E. (1990) Equivalence of finite element methods for problems in elasticity. *SIAM J. Numer. Anal.*, **27**, 1486–1505.

Grisvard, P. (1992) *Singularities in Boundary Value Problems*. Recherches en Mathématiques Appliquées [Research in Applied Mathematics], vol. 22. Masson, Paris, Berlin: Springer.

Gudi, T. (2010) A new error analysis for discontinuous finite element methods for linear elliptic problems. *Math. Comp.*, **79**, 2169–2189.

Guzmán, J. & Neilan, M. (2014) Conforming and divergence-free Stokes elements on general triangular meshes. *Math. Comp.*, **83**, 15–36.

Hu, J., Ma, R. & Shi, Z. C. (2014) A new a priori error estimate of nonconforming finite element methods. *Sci. China Math.*, **57**, 887–902.

Kouhia, R. & Stenberg, R. (1995) A linear nonconforming finite element method for nearly incompressible elasticity and Stokes flow. *Comput. Methods Appl. Mech. Eng.*, **124**, 195–212.

Neilan, M. & Sap, D. (2016) Stokes elements on cubic meshes yielding divergence-free approximations. *Calcolo*, **53**, 263–283.

Schedensack, M. (2017) Mixed finite element methods for linear elasticity and the Stokes equations based on the Helmholtz decomposition. *ESAIM Math. Model. Numer. Anal.*, **51**, 399–425.

Stenberg, R. (1987) On some three-dimensional finite elements for incompressible media. *Comput. Methods Appl. Mech. Eng.*, **63**, 261–269.

Stenberg, R. (1990) A technique for analysing finite element methods for viscous incompressible flow. *Int. J. Numer. Methods Fluids*, **11**, 935–948. The Seventh International Conference on Finite Elements in Flow Problems (Huntsville, AL, 1989).

Verfürth, R. (2013) *A Posteriori Error Estimation Techniques for Finite Element Methods.* Numerical Mathematics and Scientific Computation. Oxford: Oxford University Press.

Zhang, S. (2005) A new family of stable mixed finite elements for the 3D Stokes equations. *Math. Comp.*, **74**, 543–554.